The Influence of Corrosion Inhibitors on Hydrate Formation Temperature along the Subsea Natural Gas Pipelines

E.O. Obanijesu[1]*, R. Gubner[2], A. Barifcani[3], V. Pareek[1] and M.O. Tade[1]

1. Department of Chemical Engineering, Curtin University, Bentley Campus, Perth, W.A. 6102, Australia
2. Corrosion Centre for Education, Research & Technology (CORR-CERT), Curtin University, Bentley Campus, Perth, W.A. 6102, Australia
3. Clean Gas Technology Australia Research Centre (CGTA), Curtin University, Bentley Campus, Perth, W.A. 6102, Australia

ABSTRACT

Pipeline industry annually invests millions of dollar on corrosion inhibitors in order to minimize corrosion's implication on flow assurance; however, attention has never been focused on the possibilities of these chemicals to promote hydrate formation along deepwater pipeline which is also a flow assurance problem. Five inhibitors were investigated in this study at different concentrations and pressures in a cryogenic sapphire cell at static condition. The changes in the formation temperature established that all the inhibitors promote hydrate but at different rates while their hydrate formation patterns also differ from one another. Their ability to promote hydrate could be attributed to their hydrogen bonding properties which is required for hydrate formation. Also, the difference in the promotion rate is attributed to their different sizes and structures, active functional groups and affinity for water molecules which determine the type of hydrogen bonding exhibited by each inhibitor while in solution. The structure and size of each inhibitor also affect its electronegativity and ionization energy since the active electrons of some of the inhibitors have direct exposure to the nucleus while for others; the active electrons at the outermost shell have been shielded from direct influence of the attractive force. Furthermore, the active functional groups obeys electronegativity trend of periodic table to determine whether the resulting bond type will be polar ionic, covalent or ionic with some covalent characteristic in nature. Though, all the inhibitors are foamy; Dodecylpyridinium chloride (DPC) was however the foamiest. DPC also exhibited its highest promotion ability at 200ppm and exhibited specific behaviour at 5000ppm to suggest a change in the hydrate formation rate beyond the critical micelles concentration (CMC). Again, increase in agitation rate prolonged the complete solidification time of the hydrates probably due to the gas solubility. Finally, the feasibility of using this chemical as an additive at high concentrations for natural gas transportation and storage in slurry form was observed due to some exhibited properties, this however requires further investigations.

Keywords: CO_2 Corrosion inhibitors; Gas hydrate; Formation temperature; Subsea pipelines; Surfactant; Hydrogen bonding; Structural size distribution.

*** Correspondence Author**
E-mail address: e.obanijesu@curtin.edu.au; emmanuel257@yahoo.com
Tel: +61414512670

1 INTRODUCTION

Inhibition of corrosion along the inner wall of pipelines during natural gas transportation is a major investment in the gas industry due to the implications of the corrosion problems on flow assurance. In fact, natural gas pipelines, which are vastly manufactured from low-carbon steel materials for cheaper cost implications (Papavinasam et al, 2007) are susceptible to sweet corrosion due to availability of the carbon-dioxide and water molecules within the gas flows (Gaverick 1994). This corrosion type is responsible for 60% of oil and gas field failures (Lopez et al, 2003) while the annual global cost on economic and capital losses from corrosion is estimated to be in excess of AU$2.2 trillion. In view of this, to minimize the impacts on flow assurance, corrosion inhibitors are injected as different chemical compounds into the pipelines during the gas transportations and various researches have been funded to improve the performance of these chemicals.

Corrosion inhibitors are generally organic and inorganic compounds and they operate by being either anodic or cathodic in nature (Aljourani et al, 2009). While the anodic inhibitors form a passivation layer on the metal surface thus preventing its oxidation, the cathodic inhibitors retard the corrosion by inhibiting the reduction of water to hydrogen gas. The suitability of each chemical depends on the pipe's material of construction, the gas composition and the operating conditions. The efficiency of each inhibitor is influenced by the operating conditions and material properties (Doner et al, 2011). The operating conditions influence the corrosion rate and the inhibitor properties determine its effectiveness. The operating conditions include temperature, pressure, pH, inhibitor concentration, flow rate and CO_2 concentration (Abdel-Gaber and Saadawy, 2013; Liu et al, 2013) and the inhibitor properties include the alkyl chain length, ring size, type of head, bond type, bond strength, contact angle, and unit cell structure and parameters (Shaban et al, 2013).

Corrosion inhibitors generally possess surfactants properties (El-Mahdy et al, 2013) and surfactants have been established to aid hydrate formation (Mandal and Laik, 2008). Hydrate formation is one of the major flow assurance problems in pipeline engineering; it annually costs the gas industry millions of dollars for its minimization and billions of dollars on the eventual consequences (Obanijesu et al, 2011). Gas hydrates are ice-shaped, crystal lattice, solid compounds formed by the physical combination of water molecules with small paraffinic homologous hydrocarbon molecules (C_1-C_4) and the non-hydrocarbon components (CO_2, H_2S, N_2, etc) at high pressure and low temperature due to the weak Van der Waals forces and the hydrogen bonding properties of water (Chapoy et al, 2010; Zhang et al, 2011). The crystalline compound is stabilized by the encapsulated smaller molecular diameters guest such as CH_4 and C_2H_6 (Sloan and Koh, 2007) which are trapped in the microcavities of a crystal lattice provided by the host water. Gas hydrate formation during deepwater transportation is aided by the favourable thermodynamic conditions of the producing environment. If not quickly removed, the hydrate grows and accumulates along the line to block the inner orifice of the pipe thus leading to pressure build-up and eventual pipeline rupture.

Several studies have been carried out on properties and efficiencies of various corrosion inhibitors (Bentiss et al, 2000; Aljourani et al, 2009) but none of the existing literature have investigated the ability of these chemicals to promote hydrate formation (Sloan, 2003; Gabitto and Barrufet, 2009; McConnell et al, 2012) hence, the significance of this study is to select five of the most regularly used inhibitors as listed in Table 1 to investigate the capability of them for promoting hydrate formation along deepwater gas pipelines.

2 METHODOLOGY

2.1 Reagent, Materials and Equipment

The corrosion inhibitors investigated are presented in Table 1 while Table 2 shows the natural gas as prepared by BOC Gases, Australia (based on the authors' specifications) so as to maintain constant composition throughout the experiment. Purified water was obtained from a reverse osmosis system (Milli-Q†) as the double-distilled, ultrapure laboratory grade (MQ-H_2O). The five inhibitors were prepared from their various fresh stocks and each experiment was conducted at static condition inside a cryogenic sapphire cell (Figure 1).

The cryogenic sapphire cell equipment is made up of piston pump, pneumatic pump, sapphire cell unit, valves, two cameras and other fittings. The equipment was manufactured by ST (Sanchez Technology) in France and operates at a temperature range of -160^{o}C – 60^{o}C (with accuracy of ± 0.10^{o}C) and pressure range of 1bar – 500bar (with accuracy of ± 0.5bar). The cell uses the already in-built softwares (namely, Falcon-E4378-Curtin-Cryogenic Cell, Workbench V-5-Gas pump-Pressure software and Texmate Meter Viewer) to monitor and regulate the operating temperature and pressure of the system.

The sapphire cell unit (Figure 2) is an inner glass cell of 60ml for liquid/gas interaction and has a magnetic stirrer which could be regulated to a desired speed. A thermocouple is placed on the top of the cell to read the gas phase temperature (or TOP TEMPERATURE) and another to the bottom to read the liquid phase temperature (or BOTTOM TEMPERATURE) during an experiment. For each experiment, the cell was properly cleaned and vacuumed in order to drastically minimize experimental errors. To achieve this, the cell is firstly depressurized by direct venting to the atmosphere followed by opening the cell door to critically clean the glass cell with MQ-H_2O. The internal wall of the glass cell was then

completely dried with air using an air blower in order to minimize water retention and the glass cell was finally secured with nuts at both ends. The cell door was then closed and securely locked while the whole cell was vacuumed and the inlet valves tightly closed.

During the experiment, the cell temperature was controlled using Falcon-E4378-Curtin-Cryogenic Cell software which was a temperature regulator with constant pressure while the cell pump was controlled for pressure regulation using Workbench V-5-Gas pump-Pressure software; the pump's motor speed was always set to 100% for utmost efficiency. Finally, the cell's temperature and pressure were monitored through the Texmate Meter Viewer software which displays the operating pressure and the temperatures (TOP and BOTTOM) inside the cell at each time. The Falcon, Workbench and Texmate Meter Viewer softwares were connected to a computer and then, the whole process is controlled and regulated properly. Progress of each experiment was monitored through the two mounted cameras attached to the Cryogenic Sapphire Cell while the generated data were automatically logged by the system.

2.2 The gas preparation for laboratory experimentation

500ml cylindrical sampling bottles, made of steel were each vacuumed with a 2-stage Edwards Rotation pump with an AC motor of 50Hz, Voltage of 220/240V and speed of 1425rpm. Each cylinder was then filled with fresh natural gas composition using a pressure transducer which is connected to power source with a cable of Type Gefion PI205. Each filled bottle is fitted to the manifold line and the whole system is again vacuumed. The gas was compressed to 100bar into the Sapphire cell through V9 (Figure 1) while 5ml of already prepared liquid phase solution was injected into the cell through V5. The liquid phase solution was either MQ-H_2O (for blank experiment or 0ppm concentration) or a required corrosion inhibitor whose concentration was prepared using Equation 1.

$$M_1V_1 = M_2V_2$$ Equation 1

All lines (including the manifold line and the piston pump) were then connected to the sapphire cell and finally vacuumed.

2.3 General Experimental Operations

The system's pressure was raised within the desired pressure (100bar for the first set of experiment) using both the booster and piston pumps while the WORKBENCH software was used to fix for specific operating pressure. The cell was heated up to 35^{o}C as a reference point temperature (thus, giving the study a baseline for data generation), the heater was then turned off and the experimental SET-POINT TEMPERATURE (T_{set}) was fixed to 10^{o}C. The chiller was then switched on and the experiment commenced. At the commencement of each experiment, the BOTTOM TEMPERATURE (T_B) and TOP TEMPERATURE (T_{Top}) were recorded. The T_B represented the temperature of the liquid phase in the cell while T_{Top} was that of the gaseous phase. As the cooling progressed, changes in the T_{Top}, T_B, and AIR BATH TEMPERATURE (T_{AB}) were automatically logged every milliseconds by the Falcon software for retrieval after each experiment. Other visual observations such as the interphase condition (clear or cloudy), the point when the wall of the sapphire cell started turning (or fully turned) cloudy; the temperature where the first hydrate particle was formed, the agglomeration, growth and behaviour; the foaming properties, the point where the stirrer stopped agitating due to complete hydrate blockage and the reduction rate of the liquid volume in the cell, were also recorded into a log-book. These data were also recorded through the video cassette recorder (VCR) incorporated into the computer software for the study. At the end of each experiment, the hydrate formation temperature was recorded while the automatically logged data were downloaded.

2.4 Initial study on Inhibitor-Hydrate Relationship

Before the commencement of the experiments, HYSYS software was used to investigate the compositional phase behaviour of the gas at different temperatures and pressures (Table 3). This was to ascertain if the gas will remain gaseous at a very low temperature and maintain a constant composition throughout the study. This was important since the experiments were to be conducted at winter period; at a very low temperature, CO_2 gas can undergo partial condensation to give the gas mixture different composition at different experiment based on the environmental conditions.

HYSYS software was also used to predict the formation temperature of the gas composition at 50 bar, 100bar and 150bar (Figure 3) to obtain a rough formation temperature point for the blank studies (pure liquid without any inhibitor). A blank experimental study was carried out to establish the hydrate formation temperature point in order to save time during the experiment. This was conducted by introducing 1200ml of the gas mixture through the manifold into the system and then pressurized with 5ml of MQ-H_2O (liquid phase) in the 60ml sapphire cell at 100bar while the temperature was gradually reduced until the first point where hydrate particle was formed. The gas/liquid mixture in the cell represents blank mixture. The value from this experiment served as the baseline temperature (T_{Blank}).

After establishing the hydrate formation temperature at blank condition, 500ppm of MP was prepared using equation (1) to form the newly desired mixture of liquid phase (blank+inhibitor). 5ml of the prepared 500ppm solution was injected into the sapphire cell through V5 while 1200ml of the gas was compressed in through V9 and the experiment was repeated at 100bar until hydrate particle is formed, this generate a new formation temperature (T_{New}). The same experimental procedure was repeated for the other inhibitors, one at a time.

The impact of each inhibitor on the hydrate formation temperature was obtained by calculating the deviation in temperature ($T_{Deviation}$) using Equation 2.

$$T_{Deviation} = T_{New} - T_{Blank} \quad \text{Equation 2}$$

To evaluate the performance of the equipment and ascertain accuracy of the generated experimental data, the blank study was repeated three times while some of the experiments (with inhibitors) were selected at random for replication; it was observed that the same results were obtained. Fluid leakage was also prevented during the experimentations in order to minimize errors. Again, parallax error was avoided during the preparation of liquid phase solutions. Furthermore, there was no fluctuation in the liquid head in the cell throughout the experiments. Statistical analysis on the generated data gave the maximum experimental error of 1.299%. This clearly showed that the data obtained were accurate within the limits of experimental errors since the probability limit (confidence level) is above 95%.

2.5 Further Studies on DPC.

The results obtained through $T_{Deviation}$ revealed that DPC had the highest deviation value; hence, the needs for further studies on the chemical due to its observed significant hydrate promotional ability. These studies were conducted at different pressure range of 50bar, 100bar and 150bar and concentration range between 0ppm and 10000ppm. These selected pressures are practically justified because many offshore transmission and distribution operations are performed around these pressures and above (Matranga et al, 1992; Derbeken, 2011, Mahgerefteh et al, 2011).

Concentration-pressure matrix study

The concentration profile for DPC was investigated in order to study the inhibitor's behaviour at different pressures and concentrations. First, concentration profile for the inhibitor at 50 bar was developed by conducting the experiment at 50bar for 1000ppm, 2000ppm, 3000ppm, 5000ppm and 10000ppm each. This wide concentration range was used for both academic and industrial applications. Industrially, 200ppm is the maximum applied concentration due to cost implication on operation; however, it is important to academically study the trend at higher concentrations in order to study the feasibility of the chemical to serve as a hydrate inhibitor at such concentration(s). For each experiment, 5ml of the prepared concentration (in ppm) and 600ml of the fresh gas were fed into the cell and the experiment carried out at 50bar until hydrate is formed. The formation temperature was recorded and the cell cleaned. The experiment was then repeated at 100bar and 150bar for each of these concentrations. 1200ml and 1500ml gas volume were introduced into the sapphire cell respectively for the experimentations at 100bar and 150bar. The hydrate formation temperatures were properly recorded, the cell cleaned after each experiment and the generated data was analysed for the Pressure-Concentration matrix. Each of these experimental points was repeated in order to ascertain the accuracy and duplicability of the results.

Location of critical/peak operating concentration

While the effectiveness of a corrosion inhibitor depends on the fluid composition, quantity of water, and flow regime; the quantity of corrosion inhibitor required within a pipeline is a function of the chemical price, pipe diameter, the length of the pipeline, the desired film thickness and, the quantity and the quality of the transported natural gas (Whited, 2003; Schlumberger, 2011). This quantity was estimated by Schlumberger (2011) as

$$V = L * D * 0.0798 * Dft$$ Equation 3

Since chemical concentration plays a critical role during gas transportation, there is therefore a need to establish the critical operating concentration. The critical (or peak) operating concentration is the concentration at which the highest formation temperature is recorded and hydrate is easily promoted along the pipeline system at this concentration (Liu et al, 2012). Operating at critical concentration should be avoided at all cost due to the safety and economic impacts on the industry. Continual operation at this concentration means that, the pipeline industry would have to invest in the continual removal of the hydrate blocks within the line in order to prevent full-bore rupture of the pipeline.

Since pressure-concentration matrix study has established that at all pressure, the formation temperature dropped between the concentrations of 500ppm and 1000ppm (Figure 18), definitely, the peak could not be within this range. Therefore, 250ppm was studied at 50bar, 100bar and 150bar in order to investigate whether the peak concentration lied between 0ppm (blank) and 500ppm. The results obtained at 250ppm for the three pressure points were higher than at 0ppm and 500ppm respectively (Figure 4). This confirmed that the critical concentration was between 0ppm and 500ppm. Therefore, the final study was carried out at 100bar for concentrations of 0ppm, 50ppm, 100ppm, 150ppm, …. 500ppm respectively.

3 RESULTS AND DISCUSSIONS

3.1 Hydrate Promotional Ability of Corrosion Inhibitors

The initial study on the five inhibitors confirmed that corrosion inhibitors generally aid the promotion of hydrate formation along deepwater natural gas pipelines by increasing the formation temperature but at different rates (Figure 5), but DPC have the highest deviation

value of 1.5^{o}C as shown in Table (4). Their general ability to promote hydrate could be due to their surfactant and hydrogen bonding properties as explained below.

Corrosion inhibitors are mostly cationic surfactants. The cationic surfactants are the most expensive and hence, rarely produced or used (Table 5) due to the high pressure hydrogenation reaction carried out during their synthesis. However, due to their ability to absorb on negatively charged substrates to produce antistatic and hydrophobant effects, they are of most value as corrosion inhibitors. Cationic surfactants dissociate in aqueous solution into anion and cation but exhibits positively charged head groups and have anti-static properties (Salagar, 2002)**.** Anti-static property of a material is its ability to minimize the generation of static charges without depending upon the material's resistivity (ESD, 2009). Surfactants have generally been established to be hydrate promoters (Gayet et al, 2005; Wu et al, 2011) and a study conducted by Karaaslan and Parlaktuna (2000) showed that cationic surfactants increase the hydrate formation rate at low concentrations. This explained why the corrosion inhibitors could promote hydrate formation since they are usually introduced into the gas pipeline at low concentrations for cost implication.

When injected into a gas pipeline system, corrosion inhibitors have their hydrophilic end adsorbed to the pipe wall because of the high intensity of their highest occupied molecular orbital (HOMO) structure while the hydrophobic end (carbon chain length) is in the gas stream. This enables the inhibitors to prevent any interaction between the water molecules in the gas stream and the pipeline, thus, inhibiting corrosion by spreading themselves throughout the entire pipe surface. At the same time, the applied inhibitor is also present in the gas stream to exhibit its surfactant behaviour. It migrates to the interface and orientates in a way that the hydrophilic end is placed in the available water while the hydrophobic end lies

in the hydrocarbon (Kuhn and Rehage, 1999; Nimlos et al, 2012). This stabilizes the gas-water mixture by reducing the surface tension at the interface between their molecules. Because the fluids do not dissolve in each other, this surfactant characteristic displayed by the inhibitor keeps the entire mixture from separating into layers, thus, affecting surface characteristics of the system by increasing the contact of the two fluids (wettability). Through this, the hydrophobic end within the gas stream encourages the gas components to dissolve more into the water available molecules. This result in strong interaction between the carbon molecules in the corrosion inhibitor and that of the methane present in the gas stream (Daimaru et al, 2007). At this very point, hydrogen bonding is the only missing link for hydrate to form and it is readily supplied by the hydrogen-bonded water molecules which will cluster with the solutes of the hydrocarbon gas to form hydrate crystals at certain concentration and size (Vysniauskas and Bishnoi, 1983; Zhong and Rogers, 2000). The two hydrogen atoms in each water molecule are separated at an angle of 108^{o} due to the hydrogen bonds formed with oxygen (Carroll, 2009); this results in the formation of polyhedral cavities between several water molecules. The solute molecules in the gas (e.g. CH_4, CO_2, etc) are then trapped within the cavities to form the required hydrate type (Figure 6).

Like water, all corrosion inhibitors also exhibit hydrogen bonding properties in their solid and/or liquid states. Hydrogen bonding ability of MP, CPC, DPC, TB and BDHC are respectively reported by Ma et al (2005), Okazaki et al (1976), Akba and Batigoc (2008), Saeed et al (2011) and Al-Kady et al (2011). The contributed hydrogen-bonding from each inhibitor will determine the resulting polyhedral types, hence, the types of hydrate that would be formed based on the individual properties such as size and bond angle size amongst others.

3.2 Inhibitors' varied promotional rates on the Hydrate Formation Temperature

At the same operating conditions (including inhibitor concentration, liquid volume and operating pressure), the results obtained showed that corrosion inhibitors promote the hydrate formation at different rates with the trend as DPC > BDHC > MP > CPC > TB (Figure 7). This characteristic may depend on cumulative effects of many factors such as their sizes and structural distributions, active functional groups and affinity for water molecules which eventually impact on their hydrogen bonding properties and electronegativity as thus discussed.

As cationic amphiphiles molecules, corrosion inhibitors possess polar and non-polar ends. The polar end contains heteroatom(s) such as O, S, P, or N which determines the type(s) of hydrogen bonding exhibited while in solution, and whether the formed bonding will be polar covalent, ionic or ionic with covalent character in nature. This polar end is however attached to the non-polar hydrocarbon chains (apolar end) which enable the inhibitor to form onium and counterion structures (Vongbupnimit et al, 1995). The different sizes of the apolar end give them structures that are responsible for their different molecular aggregations, thus, giving each inhibitor unique chemical, physical and other phenomena ability. Thus, depending on the structure and size of the apolar end, the active electrons (the polar end) at the outermost shell for some inhibitors are allowed to have direct exposure to the nucleus while the electrons are shielded for other inhibitors. The distance between the active atom(s) at the outermost shell and the nucleus of a substance affects its electronegativity and affinity for water.

Electronegativity is a function of atomic radius and number of electrons in the outermost shell; the higher the electronegativity, the stronger the bond type. The farther the electrons

attached to the outermost shell from the influence of the nucleus charge, the easier it is to draw it away and the weaker the hydrogen bond that could be formed. The types and strength of the resulting hydrogen bonding will impact the average bond length, bond angle, the molecular packing and the torsion angles. The affinity of each inhibitor for water molecules affects its level of promotion; the more the affinity, the more the promotion ability. This affects the inhibitor's hydration ability to forming more hydrogen bond with water by taking more water molecules into the complex three dimensional structures which will confine the gas into its cage (matrix) to form $X.H_2O$, $X.10H_2O$ and/or $X.50H_20$ where X is a particular inhibitor. The strength of the hydrogen bond(s) formed is/are determined by the accessibility of the hydrogen atom(s) to the required site which thus encourages electrolyte selectivity through stericity and nucleophelicity.

MP has the ability to form a dimensional chain complex due to the existence N....H hydrogen bonding (Ma et al, 2005), the inhibitor also owns a de-protonated heterocyclic thioamide group $(N\text{-}C\text{-}S)^-$ that makes it to act as an S or N-bridging ligand. While forming hydrate, the chemical (Figure 8a) serves as a bridging ligand coordinate to a crystal structure which is stabilized by N···H, O—H···O and O—H···S (Li et al, 2010). However, second-and fourth-order Moller-Plesset perturbation theory and thermodynamic perturbation theory implemented on a Monte Carlo NpT simulation have shown that the S-H bonding is more stable in gas phase while N-H type is more stable in solution (Lima et al, 2006). From their structure likewise, CPC (Figure 8b) can form N···H and H···Cl bond types; TB (Figure 8c) forms S···H and N···H; DPC (Figure 8d) forms N···H, H···O and H···Cl; and BDHC (Figure 8e) forms N···H and H···Cl.

The observed hydrate formation trend for the studied inhibitors is then justified considering the cumulative effects of the structural distribution, active functional group and affinity for water. DPC has the strongest ability because it contains both the Cl^- and N^+ groups that can react very fast with water molecules because of highly polar and strong hydrogen bonding properties which have higher affinity for water molecules to meet the required thermodynamic energy needed for the hydrate formations. BDHC also has these two groups, it however has a large non-polar part that restricts interaction with water because of increase in apolar character which involves London dispersion force (instantaneous dipole). Though, MP is expected to have more affinity for water compared with DPC due to it's readily solubility property, DPC and BDHC however show more polar character comparatively. Finally, although CPC also has Cl^- and N^+ groups in its structure and expected to be readily soluble and reactive with water like DPC; the hydrophobic end however is very large.

3.3 Hydrate Formation Patterns of the five inhibitors

The hydrate formation patterns for the blank (without inhibitor) and the five inhibitors were studied through visual observations. For blank concentration, the formed hydrate started building at the gas phase (Figure 9a) and grew gradually at the gas phase (Figure 9); while the liquid volume was gradually reducing until the lower part of the cell around the mixer became blocked (Figure 9).

The hydrate for MP initially formed thinly at the interphase without agglomerating for about 6 mins (Figure 10a); it then grew disjointedly, block by block and piece by piece at the glass surface at a very low rate. During the growth, the hydrate seemed suspended in the gas phase away from the liquid phase with the top building sky-like with snow colour (Figure 10b & c).

At the formation temperature, CPC's hydrates were initially formed at the interphase in chips (Fig 11a). They then dissolved into the liquid phase within two minutes (Figure 11b) and started growing gradually but at a slow rate until blockage (Figure 11c).

Hydrates from DPC started at the interphase (Figure 12a). For the initial 7 mins after formation, the growth was very slow (Figure 12b) but increased very sharply after (Figure 12c). The new growth rate was so alarming and the lower glass column around the mixer was completely blocked within the next 4mins while the stirrer stopped rotating within 1 min after. For this chemical, it is observed that the liquid disappearance rate and the hydrate formation rate were very much higher comparably with the other four inhibitors.

The hydrate for TB was as white as snow and formed at the interphase (Figure 13a). It then started growing upward along the cell glass column at the gas phase without mixing with the liquid phase (Figure 13b). The growth rate at the gas phase was rapid while the liquid phase was slightly turning cloudy and disappearing downward until it finally vanished. The hydrate never collapsed into the liquid phase but solidified in the gas phase and grew (Figure 13c).

The BDHC's hydrate formed at the interphase (Figure 14a) then rapidly broke into chips and mixing with the liquid phase (Figure 14b). The formed hydrate chips then grew inside the liquid as flocs, breaking up and adding up to the existing hydrates until total blockage (Figure 14c). The hydrate growth rate for this inhibitor was observed to be higher than those of the other inhibitors except for the DPC.

3.4 Outcomes of the Further Studies on DPC

3.4.1 Formation patterns at different pressures and concentrations

DPC promoted hydrate formation at all investigated concentrations for the three pressures (50, 100 and 150 bar). The liquid phase never turned cloudy until the formation period and the formed hydrates were very clear and ice-like in colour at all concentrations and pressures. Also, the hydrates started to form at the interphase and grew upwards into the gas phase. For each experiment, the liquid phase took some time to completely disappear as the hydrate turned into slurry and slowly built-up in the glass cell; however, the growth rate suddenly and sharply increased to shortly block the glass column. Figure (15) shows this phenomenon at 100 bar and 500ppm; however, this trend was observed at all pressure and concentration but with different timings.

It was further observed that the inhibitor was very foamy regardless of the concentration (Figure 16); however, the foaming ability reduced with increase in concentration except for 5000ppm. This brings the first suggests that this concentration might be the Critical Micelle Concentration (CMC) for DPC hydrates.

Also for all concentration, it was further observed that the inhibitor remained foamy even after the hydrate had totally blocked the orifice of the glass cell as shown in Figure (17).

3.4.2 Concentration-pressure matrix study on DPC

The concentration-pressure matrix study showed a unique trend by giving a similar ‘camel back’ structure at all the pressures (Figure 18). Connecting the data points generally revealed that the formation temperature increased sharply from 0ppm to 500ppm and then reduced from 500ppm to 2000ppm. It started to increase again at 3000ppm; however, a sharp increase

was noted at 5000ppm before a final drop at 10000ppm. This pattern strongly showed the effect of pressure on hydrate formation point.

The experiment for 5000ppm was repeated three times but the same result was obtained. This sharp increase may be due to the effect of change in the hydrate formation rate beyond the critical micelles concentration (CMC). According to Zhong and Rogers (2000), at a concentration above its CMC, the formation rate of gas hydrate in a static system increases in multiple times of over 700.

3.4.3 Critical Operating Concentration for DPC

This study revealed the critical operating concentration for DPC at 100bar to be 200ppm (Figure 19), thus indicating that application of this chemical within this concentration would easily aid hydrate promotion in deepwater pipeline network during gas production and transportation. In practice, inhibitors are applied in low dosage for cost minimization; all values within the experimental errors to this 200ppm should however be avoided during the transport operation since they may have the same effect, this avoidance could consequently minimize full bore rupture.

Nevertheless, DPC remains one of the most favourable chemicals commonly used in the gas industry to extend the shelf-life of process equipment through to its remarkable effectiveness to inhibit CO_2 corrosion (Wang and Free, 2003; Pandarinathan et al, 2011). Its mixed type inhibition properties allows it to inhibit corrosion by adsorbing onto the pipe's inner surface both chemically and physically (Durnie et al. 2005) through electrostatic adsorption and π-electron sharing (Likhanova et al. 2010), thus simultaneously inhibiting corrosion both at anodic and the cathodic sites.

In view of the huge importance of DPC to corrosion inhibition, balance should be struck in its utilization in order not to create hydrate formation problem.

3.4.4 Pressure Effect on Formation Temperature Point for DPC

At all concentrations, it was observed that the hydrate formation temperature increased with operating pressure as shown in Figure (20), these results perfectly agreed with the published literature (Moraveji et al, 2010; Wu et al, 2013).

After each formation, it was generally observed that the temperature dropped further below the formation temperature value before the hydrate started agglomerating, it was however observed that the temperatures at each concentration followed the trend of 50 bar < 100bar < 150 bar. This also agreed with established literature that the hydrate growth rate directly is proportional to operating pressure (DelleCase et al, 2008; Li et at, 2013). Specific observations concerning each pressure are further presented below.

3.4.4.1 Specific observation at 50 bar

At 50bar, the hydrates were independently formed in bits and 'ring shapes' at various spots, they then cycled round the glass wall at interphase while growing (Figure 21). After the formation, the temperature kept dropping while the hydrate agglomerated very slowly. At $2^{o}C$-$3^{o}C$ below the formation temperature, the temperature suddenly increased and the hydrates growth increased sharply to fill the glass orifice, block the glass and stop the stirrer within 15 minutes depending on the inhibitor's concentration; the higher the concentration, the lower the observed blockage rate.

3.4.4.2 Specific observations at higher pressures (100bar and 150bar)

Experiments for all concentrations at 100bar and 150bar followed almost the same and unique trends. For each study at these pressures, tiny hydrate flocs usually started to form from within the liquid phase but quickly rose to the interphase (this requires a very good observation to notice). With time however, the flocs dissolved back in the liquid, turning it into slurry while the floc particles became noticeable in the liquor or as the hydrate agglomerated and grew (Figure 22 a-c). The hydrates then solidify at the interphase and grew upwards along the gaseous phase (Figure 22 d-e) while the liquid disappeared downward. The growth pattern might have been influenced by concentration and pressure.

As the temperature continued to drop below the formation temperature, the hydrate slurry turned into flakes but the hydrate growth rate remained generally slow. About 0.5^{o}C below formation temperature however, the temperature started to rise again but dropped back while approaching the formation temperature. Within this period, the hydrate growth rate was noticed to increase sharply and completely block the whole glass orifice within 4-6 minutes while temperature fluctuated between 0.3^{o}C and 0.5^{o}C below the formation temperature. This trend was noticed for all concentrations except 10000ppm where the temperature dropped to 1^{o}C below the formation temperature before it started rising again. Again, at 10000ppm for both 100bar and 150bar, it was observed that at some point, the formed hydrate collapsed inside the liquid and started rebuilding and growing until the blockage time (Figure 23).

3.4.5 Effect of Agitation

It was further observed that increase in agitation (stirring) rate could prolong the hydrate growth rate. At 150bar as an example, when the rate was very slow, the hydrate was formed at 17.3^{o}C; however, when the rate was significantly increased, the flocs dissolved into the

liquid completely and later started to form again at 16^{o}C. This might have to do with the combined influences of pressure, temperature, agitation and particle size on the gas solubility which could be explained using kinetic theory. According to kinetic theory, reduction in kinetic energy was experienced by the gas-liquid system as temperature dropped towards the hydrate formation point. This resulted in reduction in the molecules' motion that eventually led to reduction in the rate at which the gas molecules escaped from the solution since there was already a reduction in the rate that the intermolecular bonds broke up. This effectively increased the gas solubility. The gas solubility was further enhanced by the high pressure (150bar) at which the study was conducted. At this high pressure, Henry's Law was obeyed and the gas molecules were further pushed into the liquid; hence, the initially obtained hydrate formation temperature of 17.3^{o}C.

When the agitation rate was increased however, the solubility now depended on the particle size. The existing fine hydrate particles had more exposed surface area to the surrounding solvent. The solute (hydrate particles) then dissolved rapidly into the liquid since agitation brought the available fresh solvent into contact with the surface of the solute. As the temperature dropped further to 16^{o}C, another hydrate formation temperature was reached based on the new agitation rate. At this point, the hydrate agglomerated and grew to form an 'ice' that blocked the glass orifice.

Agitation and particle size can only affect the solute (hydrate) dissolution rate but cannot influence the saturation point, this phenomenon could further be investigated as related to deepwater natural gas pipeline in order to understand the hydrate growth process.

3.4.6 5000ppm as the Likely Critical Micelle Concentration (CMC) for DPC Hydrates

For all investigated pressures, experimental results at 5000ppm hardly followed the observed trend when compared with other concentrations. Unlike other concentrations, the formed hydrate at 5000ppm did not completely block the glass orifice; it remained as ice-flake while other concentrations formed ice-block. Thus, while the stirrer stopped agitating for other concentrations at the blockage point, it kept on rotating for each of the experiments at 5000ppm even after all the liquid had turned into hydrate. Also, an abnormal sharp increase was observed at the concentration during concentration-pressure matrix as shown in Figure (20). These differential results at this concentration showed that the chemical possesses special properties at 5000ppm which could be interpreted to be the Critical Micelle Concentration (CMC) for the chemical in hydrate conditions.

Critical Micelle Concentration (CMC) is that concentration where all the available molecules of a surfactant in solution go into micellization. Micellization is the submicroscopic aggregation of surfactant molecules (DPC for this study) that are dispersed in a liquid colloid. The aggregation is formed at each polar end of the molecules that is in direct contact with the surrounding liquid to form micelles, and this leads to sequestration of existing hydrophobic tails within the micelle centre. These polar ends are capable of forming hydrogen bonding. The shape and size of each micelle is determined by the molecular geometry of the surfactant molecules and the solution's conditions such as the pH, temperature, surfactant concentration, and the ionic strength. For any given surfactant, CMC is strongly dependant on temperature, pressure and concentration (Hara et al, 2004; Metha et al, 2005). Surface tension is strongly influenced below CMC but remains relatively constant once CMC is reached. Korotkikh and Kochurova (2006) gave the CMC value for DPC at 20^0C, 25^0C, 30^0C, 35^0C and 40^0C as $1.78*10^{-2}$M, $1.75*10^{-2}$M, $1.36*10^{-2}$M, $1.97*10^{-2}$M and $2.15*10^{-2}$M respectively.

3.4.7 Proposed feasibility of using DPC to aid natural gas transportation and storage

The results obtained revealed that the hydrate promotion ability for DPC reduced with increase in operating pressure (Table 6). At each pressure, it was further observed that the liquid disappearance rate decreased with increase in the chemical concentration (Table 7). Likewise, the hydrate growth rate followed the same trend. This suggests the feasibility of using this chemical to aid the transportation and storage of natural gas in slurry form. However, further studies should be carried out on this due to pressure effects.

For both 100bar and 150bar, the blockage time decreases with increase in concentration. At 100bar for instance, it was observed that at 1000ppm, the stirrer stopped working due to total blockage of the glass orifice at 18minutes after formation time whereas, the stirrer stopped at 28 minutes and 32 minutes respectively for 5000ppm and 10000ppm respectively. This means that at very high concentration, DPC exhibited some hydrate inhibition properties which suggests its ability as a useful additive for natural gas transportation in slurry form. However, extensive studies should also be conducted to investigate this feasibility further.

4 CONCLUSIONS

This study has established the ability of corrosion inhibitors to promote hydrate formation along the deepwater gas pipelines and this has strong consequences on flow assurance policy of the industry through creation of one problem while solving the other. It also showed that the inhibitors promote the hydrate at different rates probably based on their structural distributions, active functional groups and affinity for water molecules which ultimately impact on their hydrogen bonding properties and electronegativity properties. Hydrates from DPC were found to be most significant and very foamy at all investigated concentrations and pressures. This specifically showed that some surfactant properties of the chemical were highly influential during the formation process.

It was further observed that this foaming ability decreased with concentration except at 5000ppm where anomalous behaviour was generally observed probably due to the CMC influence. Again, the study revealed that gas solubility during hydrate formation is influenced by pressure, temperature, agitation and particle size. Finally, DPC prolonged the total blockage of the glass orifice at 10000ppm at all pressures. There might be a need to further investigate this property as it could suggest the possibility of applying the chemical as an additive for natural gas transportation and storage in slurry form. It may further suggest the feasibility of the chemical to act both as corrosion and hydrate inhibitors at very high concentrations during the gas transportation along offshore pipeline. This may be cost effective on the long run.

Essentially, this study has brought a new focus to corrosion-hydrate relationship as well as establishing the need for further investigation on the growth and dissociation rates.

ACKNOWLEDGEMENT

The authors acknowledge the financial support from Curtin University, Perth and Western Australian Energy Research Alliance (WAERA) through the Curtin Strategic International Research Scholarship (CSIRS) and Australia-China Natural Gas Technology Partnership Fund Top-up Scholarship schemes respectively. Also, the technical support of Mr. Saif Ghadhban during the experiments is acknowledged. Furthermore, Ketrrina Lephova and Kriti Bhardwaj of CORR-CERT are acknowledged for preparing the corrosion inhibitors. Finally, Dr. Shahin Hosseini is acknowledged for providing comments during the script preparation.

ABBREVIATION LIST

$V = Vol\ (liter)$

$L = Pipe\ length\ (km)$

$Dft = Desired\ film\ thickness\ (ml)$

M_1= Concentration of available Inhibitor (ppm)

M_2=Concentration of required Solution (ppm)

V_1=Volume of Inhibitor (ml)

V_2=Volume of Solution (ml)

T_{Blank} = Formation temperature for the blank experiment

T_{New} = Formation temperature for (blank + Inhibitor).

REFERENCES

Abdel-Gaber, A.M. and Saadawy, M. (2013), "The Inhibitive Effect of a (1,3-Dioxolan-2-ylmethyl)–triphenyl phosphonium bromide on the Corrosion of Steel in 0.5 M Phosphoric Acid Solution", *Int. J. Electrochem. Sci*.,Vol. 8, pp. 2080-2094

Akba, H. and Batigoc, C.D. (2008), "Micellization of Dodecylpyridinium Chloride in Water–Ethanol Solutions", *Colloid Journal*, Vol. 70, pp.127–133.

Aljourani, J. Raeissi, K. and Golozar, M.A. (2009), "Benzimidazole and its Derivatives as Corrosion Inhibitors for Mild Steel in 1M HCl Solution", *Corrosion Science*, Vol. 51, pp. 1836–1843

Al-Kady, A.S., Gaber, M., Hussein, M.M. and Ebeid, E.M. (2011), "Nanostructure-loaded Mesoporous Silica for Controlled Release of Coumarin Derivatives: A Novel Testing of the Hyperthermia Effect", *European Journal of Pharmaceutics and Biopharmaceutics*, Vol. 77, pp. 66–74.

Bentiss, F., Traisnel, M. and Lagrenee, M. (2000), "The Substituted 1,3,4-oxadiazoles: a New Class of Corrosion Inhibitors of Mild Steel in Acidic Media", *Corrosion Science*, Vol. 42, pp. 127-146.

Carroll, J.J. (2009), "Natural Gas Hydrates - A Guide for Engineers", 2nd Edition, Gulf Professional Publishing, USA.

Chapoy, A., Haghighi, H., Burgass, R. and Tohidi, B. (2010), "Gas Hydrates in Low Water Content Gases: Experimental Measurements and Modelling using the CPA Equation of State, *Fluid Phase Equilibria*, Vol. 296, pp. 9–14

Daimaru, T., Yamasaki, A. and Yanagisawa, Y. (2007), "Effect of Surfactant Carbon Chain Length on Hydrate Formation Kinetics", *Journal of Petroleum Science and Engineering*, Vol. 56, pp. 89–96.

DelleCase, E., Geraci, G., Barrios, L., Estanga, D., Domingues, R. and Volk, M. (2008), "Hydrate Plugging or Slurry Flow: Effect of Key Variables", *Proceedings of the 6th International Conference on Gas Hydrates*, Vancouver, July 6–10.

Derbeken, J.V. (2011), "Utilities: Major PG&E Gas Line Ruptures During Hydro Test", Hearst Communications Inc., New York. Accessed on 28th December 2011 from http://articles.sfgate.com/2011-10-25/news/30322862_1_pg-e-officials-longitudinal-seam-compressor-station

Doner, A., Solmaz, R., Ozcan, M., and Kardas, G. (2011), "Experimental and Theoretical Studies of Thiazoles as Corrosion Inhibitors for Mild Steel in Suphuric Acid Solution", *Corrosion Science*, Vol. 53, pp. 2902-2913.

Durnie, W., De Marco, R., Kinsella, B., Jefferson, A. and Pejcic, B. (2005), "Predicting the Adsorption Properties of Carbon Dioxide Corrosion Inhibitors Using a Structure-Activity Relationship", *Journal of the Electrochemical Society*, Vol. 152, pp. B1-B11.

El-Mahdy, G.A., Atta, A.M. and Al-Lohedan,H.A. (2013), "Water Soluble Nonionic Rosin Surfactants As Corrosion Inhibitor of Carbon Steel in 1M HCl", *Int. J. Electrochem. Sci*., Vol. 8, pp. 5052-5066

ESD, 2009. "Electrostatic Discharge", Glossary of ESD Terms, Accessed on 28th August, 2011 from http://www.interfacebus.com/glossary-of-terms-esd-definition.html
Safety/Precaution issues.

Gabitto, J. and Barrufet, M. (2009), "Gas Hydrates Research Programs: An International Review", FINAL REPORT, CONTRACT NUMBER: DE-FG26-06NT42746, US Department of Energy, pp. 1-82

Gaverick, L. (1994), "Corrosion in the Petrochemical Industry", 1st Edition, *ASM International*, Metal Park, Ohio, USA.

Gayet, P., Dicharry, C., Marion, G., Graciaa, A., Lachaise, J. and Nesterov, A., (2005), "Experimental Determination of Methane Hydrate Dissociation Curve up to 55 MPa by using a Small Amount of Surfactant as Hydrate Promoter", *Chemical Engineering Science*, Vol. 60, pp. 5751-5758.

Hara, K., Baden, N. and Kajimoto, O. (2004), "Pressure Effect on Water Solvation Dynamics in Micellar Media", *Journal of Physics: Condensed Matter*, Vol. 16, pp. 1207–1214.

Karaaslan, U. and Parlaktuna, M. (2000), "Surfactants as hydrate promoters?", *Energy & Fuels*, Vol. 14, pp. 1103-1107

Korotkikh, O.P. and Kochurova, N.N. (2006), "Micelle Formation in Aqueous Dodecylpyridinium Chloride", *Russian Journal of Applied Chemistry*, Vol. 79, pp. 1204 - 1206.

Kuhn, H. and Rehage, H. (1999), "Molecular Dynamics Computer Simulations of Surfactant Monolayers: Monododecyl Pentaethylene Glycol at the Surface between Air and Water", *J. Phys. Chem. B*, Vol. 103, pp. 8493-8501

Li, B., Li, W., Ye, L., Hou, G.F. and Wu, L.X. (2010), "Metal-Organic Compounds: Poly[di-l2-aqua-l4-chlorido-l4-(2-mercaptopyrimidine-4,6-diolatoj4O:O:O0:O0)-disodium(I)], *Acta Cryst.*, Vol. E66, pp. 1-5

Li, W., Gong, J., Lu, X., Zhao, J., Feng, Y. and Yu, D. (2013), "A Study of Hydrate Plug Formation in a Subsea Natural Gas Pipeline using a Novel High-Pressure Flow Loop", *Petroleum Science*, Vol. 10, pp. 97-105.

Likhanova, N. V., Dominguez-Aguilar, M. A., Olivares-Xometi, O. and Nava-Entzana, N. (2010), "The Effect of Ionic Liquids with Imidazolium and Pyridinium Cations on the Corrosion Inhibition of Mild Steel in Acidic Environment", *Corrosion Science*, Vol. 52, pp. 2088-2097.

Lima, M.C.P., Coutinho, K., Canuto, S. and Rocha, W.R. (2006), "Reaction Mechanism and Tautomeric Equilibrium of 2-Mercaptopyrimidine in the Gas Phase and in Aqueous Solution: A Combined Monte Carlo and Quantum Mechanics Study, *J. Phys. Chem.*, Vol. 110, pp. 7253-7261.

Liu, J., Pan, H., Zhou, Y. and Zhou, L. (2012), "Formation Pressure of Ethylene Hydrates in Carbon Pores at Near-Critical Temperatures", *J. Chem. Eng. Data*, Vol. 57, pp 2549–2552

Liu, M., Wang, J.Q. and Ke, W. (2013), "Effect of Temperature and H_2S Concentration on Corrosion of X52 Pipeline Steel in Acidic Solutions", *Materials Science Forum*, Vol. 743-744, pp. 589-596

Lopez, D. A., Perez, T. and Simison, S. N. (2003), "The Influence of Microstructure and Chemical Composition of Carbon and Low Alloy Steels in CO_2 Corrosion: A State of the Art Appraisal", *Materials and Design*, Vol. 24, pp. 561-575.

Ma, C., Shi, Y. and Jiang, Q. (2005), "Syntheses, Characterizations and Crystal Structures of New Triorganotin Complexes with 2-Mercaptopyrimidine and 4-amino-2-Mercaptopyrimidine", *Heteroatom Chemistry*, Vol. 16, pp. 69-75

Mahajan, D., Taylor, C.E. and Mansoori, G.A. (2007), "An Introduction to Natural Gas Hydrate/Clathrate: The Major Organic Carbon Reserve of the Earth", *Journal of Petroleum Science and Engineering*, Vol. 56, pp. 1–8.

Mahgerefteh, H., Jalali, N. and Fernandez, M.I. (2011), "When Does a Vessel Become a Pipe?", *AIChE J*, Vol. 57, pp. 3305-3314.

Mandal, A. and Laik, S. (2008), "Effect of the Promoter on Gas Hydrate Formation and Dissociation", *Energy & Fuels*, Vol. 22, pp. 2527–2532

McConnell, D.R., Zhang, Z. and Boswell, R. (2012), "Review of Progress in Evaluating Gas Hydrate Drilling Hazards", *Marine and Petroleum Geology*, Vol. 34, pp. 209–223

Metha, S.K., Bhasin, K.K., Chauhan, R. and Dham, S. (2005), "Effect of Temperature on Critical Micelle Concentration and Thermodynamic Behavior of Dodecyldimethylethylammonium Bromide and Dodecyltrimethylammonium Chloride in Aqueous Media", *Colloids and Surfaces A: Physicochemical and Engineering Aspects*, Vol. 255, pp. 153-157

Moraveji, M.K., Sadeghi, A., Fazlali, A. and Davarnejad, R. (2010), "Effect of an Anionic Surfactant on the Methane Hydrate Formation: Induction Time and Stability", *World Applied Science Journal*, Vol. 9, pp. 1121-1128.

Nimlos, M.R., Beckham, G.T., Matthew, J.F., Bu, L., Himmel, M.E. and Crowley, M.F (2012), "Binding Preferences, Surface Attachment, Diffusivity, and Orientation of a Family 1 Carbohydrate-Binding Module on Cellulose", *The Journal of Biological Chemistry*, Vol. 287, pp. 20603-20612.

Obanijesu, E.O., Pareek, V., Gubner, R. and Tade, M.O. (2011), "Hydrate Formation and its Influence on Natural Gas Pipeline Internal Corrosion", *NAFTA Journal*, Vol. 62, pp. 164-173

Okazaki, M., Hara, I. and Fullyema, T. (1976), "Spectroscopic Studies of Surfactant Solubility. 1. Formation of Hydrogen Bonding between Surfactants and Chloroform", *The Journal of Physical Chemistry*, Vol. 80, pp. 64-68

Pandarinathan, V., Lepková, K. and Gubner, R. (2011), "Inhibition of CO_2 Corrosion of 1030 Carbon Steel Beneath Sand-Deposits", Paper 11261, *CORROSION 2011 Conference & Expo*, NACE International, Houston, USA, March 13 - 17

Papavinasam, S., Doiron, A., Panneerselvam, T. and Revie, R.W. (2007), "Effect of Hydrocarbons on the Internal Corrosion of Oil and Gas Pipelines", *Corrosion*, Vol. 63, pp. 704-712.

Saeed, A., Erben, M.F., Shaheen, U. and Flörke, U. (2011), "Synthesis, Structural and Vibrational Properties of 1-(4-Fluorobenzoyl)-3-(Isomeric Fluorophenyl)thioureas", *Journal of Molecular Structure*, Vol. 1000, pp. 49–57

Salagar, J.L. (2002), "Surfactants: Types and Uses – Teaching Aid in Surfactant Science and Engineering", Laboratory of Formulation, Interfaces, Rhelogy and Processes, Version #2, FIRP Booklet #E300-A, Universidad De Los Andes, Merida-Venezuela.

Schlumberger (2011), "Corrosion Inhibitor KI-3882* High Film Persistent, Batch-type Corrosion Inhibitor Designed to Control Corrosion in Oil Production Systems", Houston Texas, U.S.A, pp 1-2. Accessed on 3rd March 2013 from http://www.slb.com/~/media/Files/miswaco/product_sheets/ki_3882.ashx

Shaban, S.M., Saied, A., Tawfik, S.M., Abd-Elaal, A. and Aiad, I. (2013), "Corrosion Inhibition and Biocidal Effect of Some Cationic Surfactants Based on Schiff Base", *Journal of Industrial and Engineering Chemistry*, Vol. 19, pp. 2004-2009

Sloan, E.D. (2003), "Fundamental Principles and Applications of Natural Gas Hydrates", *Nature, Vol.* 426, pp. 353-363

Sloan, E. D. and Koh, C.A. (2007), "Clathrate Hydrates of Natural Gases", 3rd Edition, CRC Press, USA.

Surovetseva, D., Barifcani, A. and Amin, R. (2009), "Cryogenic Condensation Capture of Cr_2 from IGCC Flue Gases", CO_2CRC Research Symposium, Coolum, Queensland, Australia, pp. 1-5.

Vongbupnimit, K., Noguchi, K. and Okuyama, K. (1995), "Organic Compounds: 1-dodecylpyridinium Chloride Monohydrate", *Acta Crystallographica* Section C, Crystal Structure Communications, Vol. 51, pp. 1940-1941

Vysniauskas, A. and Bishnoi, P.R. (1983), "A Kinetic Study of Methane Hydrate Formation", *Chemical Engineering Science*, Vol. 38, pp. 1061- 1072.

Wang, W. and Free, M.L. (2003), "Prediction and Measurement of Mild Steel Corrosion Inhibition by Alkyl Pyridinium Chloride and Alkyl Trimethyl Ammonium Bromide Surfactants in Acidic Chloride Media", *Anti-Corrosion Methods and Materials,* Vol. 50, pp. 186-192.

Whited, T. (2003), "Use of Corrosion Inhibitors for Control of Corrosion in Double Bottom AST's", Praxair Services, Inc. (PSI), Broomfield, CO, USA, pp 1-5. Accessed on 23rd February 2013 from http://www.cortecvci.com/Publications/Papers/AST%20Corrosion%20Inhibitor%20Process%20v2.pdf

Wu, R., Kozielski, K.A., Hartley, P.G., May, E.F., Boxall, J. and Maeda, N. (2013), "Probability Distributions of Gas Hydrate Formation', *AIChE Journal*, Vol. 59, pp. 2040-2046

Wu, Q., Gao, X. and Zhang, B.Y. (2011), "SDS Effect on $CH_4/N_2/O_2$ Hydrate Formation Rate for CMM Separation and Storage", *Advanced Materials Research*, Vol. 201-203, pp. 471-475.

Zhang, L. Burgass, R., Chapoy, A. and Bahman, B. (2011), "Measurement and Modeling of Water Content in Low Temperature Hydrate–Methane and Hydrate–Natural Gas Systems", *J. Chem. Eng. Data*, Vol. 56, pp. 2932–2935

Zhong, Y. and Rogers, R.E. (2000), "Surfactant Effects on Gas Hydrate Formation", *Chemical Engineering Science*, Vol. 55, pp. 4175-4187.

List of Tables

Table 1: The list of inhibitors used for the study

Inhibitor	Abbreviation	Molecular Formula	Mol. Wt. (g/mol)
2-mercapto pyrimidine	MP	$C_4H_4H_2S$	112.15
Cetylpyridinium chloride	CPC	$C_{21}H_{38}NCl.H_2O$	358.07
Dodecylpyridinium chloride	DPC	$C_{17}H_{30}ClN$	283.88
Thiobenzamide	TB	$C_6H_5CONH_2$	121.14
Benzl dimethyl hexadecylammonium chloride	BDHC	$CH_3(CH_2)_{15}N(CH_3)_2CH_2C_6H_5.Cl$	396

Table 2: Composition of the studied natural gas

Component	Concentration (mol %)
CH_4	70.90
C_2H_6	5.00
C_3H_8	3.00
n-C_4H_{10}	0.94
n-C_5H_{12}	0.10
N_2	0.06
CO_2	20.0

Table 3: Phase behaviour prediction of the gas composition using HYSYS software

Temperature (^oC)	Pressure (bar)		
	50	100	150
5	Gas	Gas	Gas
0	Gas	Gas	Gas
-5	Gas	Gas	Gas
-10	Gas	Gas	Gas
-15	Gas	Gas	Gas

Table 4: Formation Temperature for the Five Inhibitors at 500ppm and 100bar

	Formation temperature (^OC)		
Inhibitor	Experimental		
	Blank	Blank + Inhibitor	Deviation
MP	14.9	15.7	0.8
CPC	14.9	15.6	0.7
DPC	14.9	16.4	1.5
TB	14.9	15.4	0.5
BDHC	14.9	15.8	0.9

Table 5: The surfactant types and their global production rates (Salager, 2002)

The Surfactant Type	World Production (%)
Anionic	50
Nonionic	45
Others	5

Table 6: Hydrate promotion ability between 0ppm and 500ppm at 100bar

Pressure (bar)	Deviation (^{o}C)
50	3.8
100	1.5
150	0.7

Table 7: Time to convert 80% of liquid to hydrate at 100bar but different concentrations

Concentration (ppm)	Time (mins)
1000	5
5000	12
10000	15

List of Figures

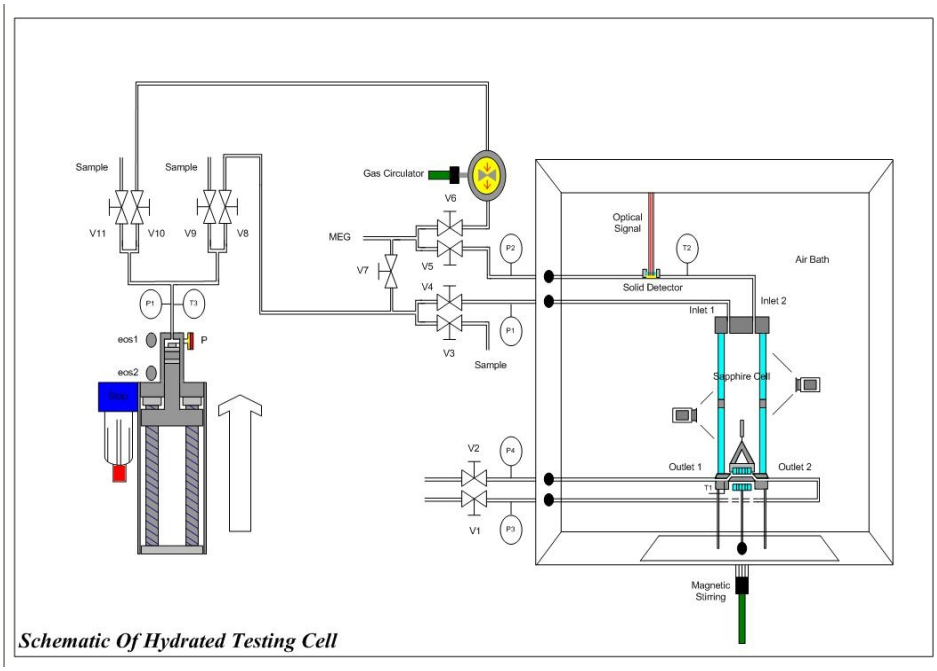

Figure 1: Schematic of the Sapphire Cell (Surovetseva et al, 2009).

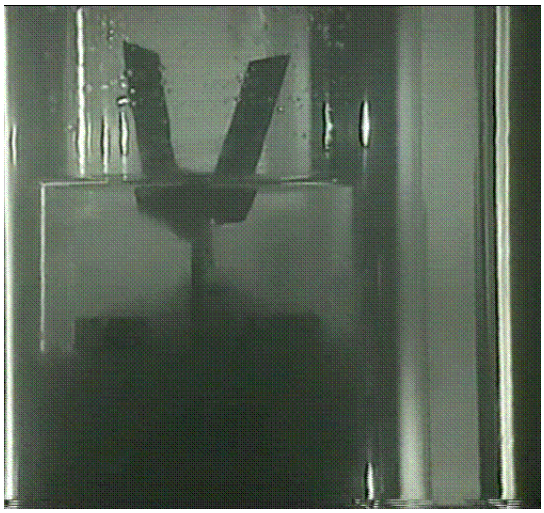

Figure 2: A typical view of liquid-gas interaction section in the sapphire cell

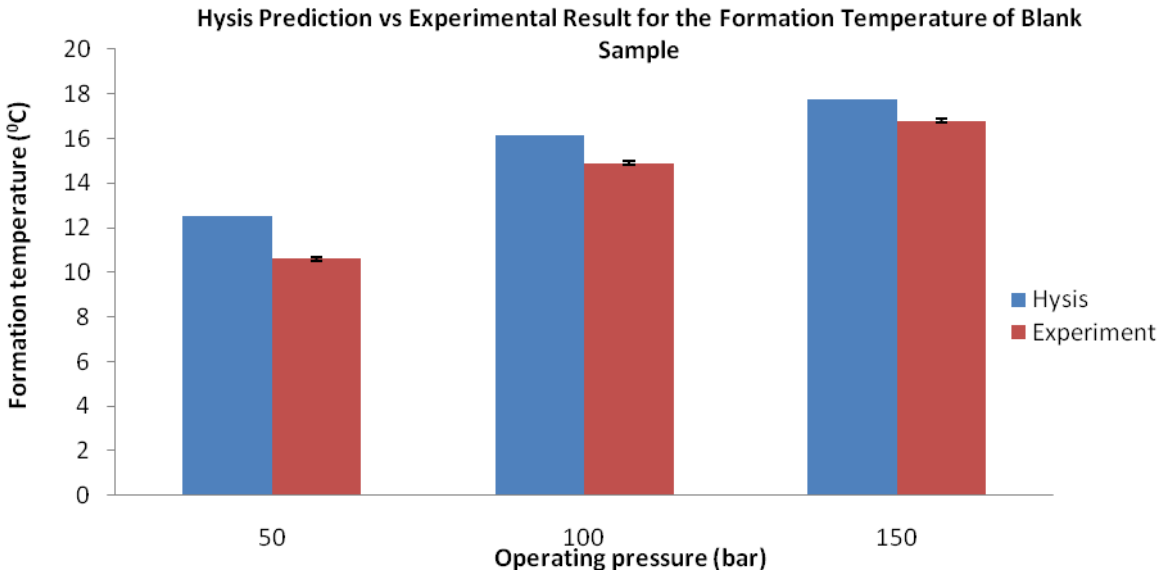

Figure 3: Blank concentration results for HYSYS prediction vs experimental result.

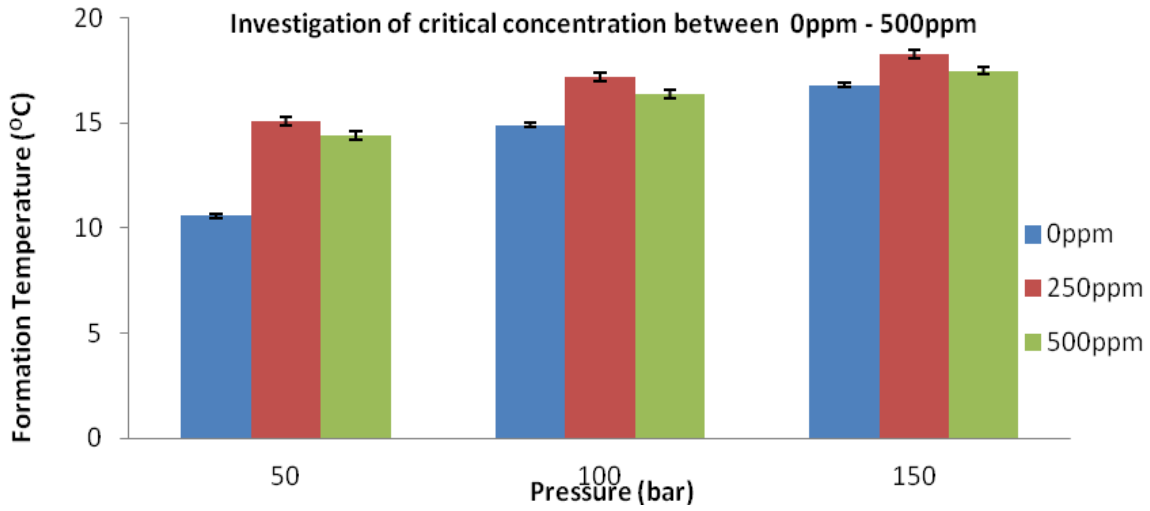

Figure 4: Investigation of the critical operating concentration for DPC.

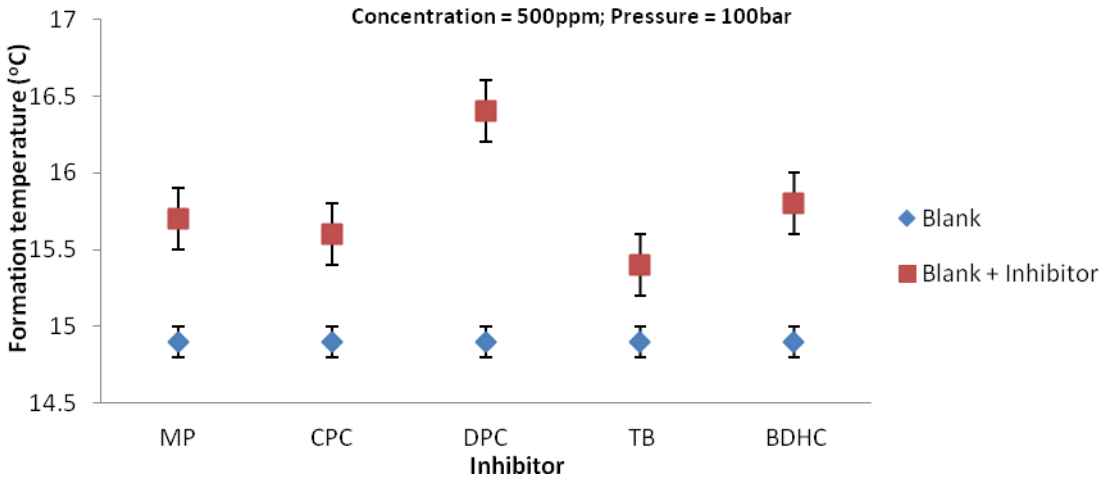

Figure 5: Hydrate formation temperature trend for the five corrosion inhibitors.

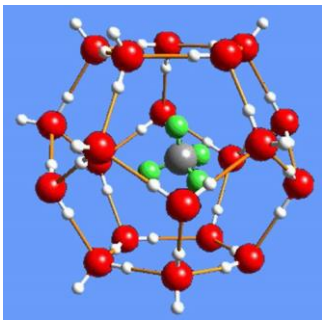

Fig. 6a: Schematic of natural gas clathrate structure where a methane molecule is encaged by a lattice of water molecules.

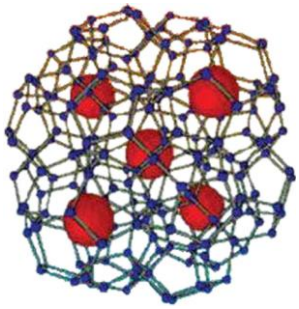

Fig. 6b: Methane clathrate dual structure.

Figure 6: Methane hydrate structures (Mahajan et al, 2007).

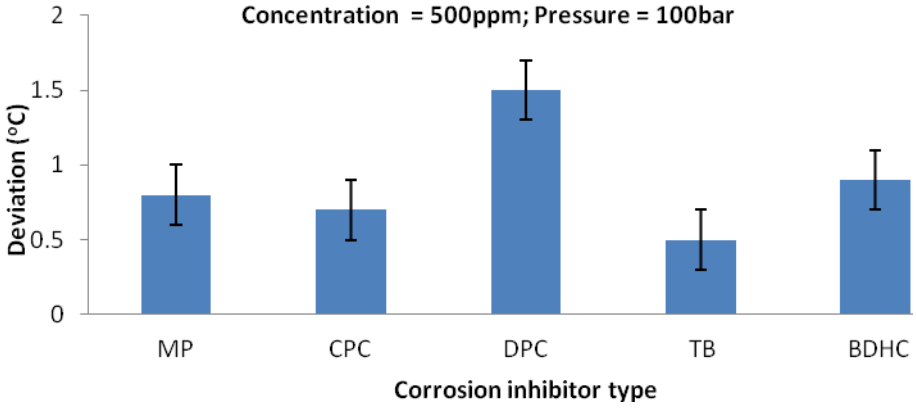

Figure 7: Formation temperature deviation of different inhibitors.

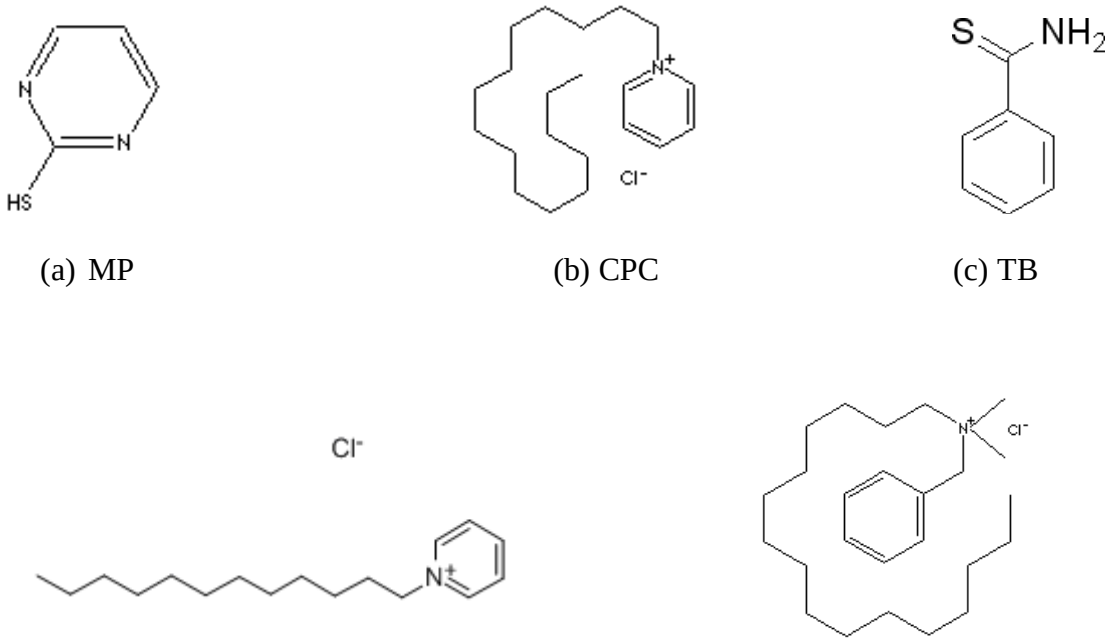

(a) MP (b) CPC (c) TB

(d) DPC (e) BDHC.

Figure 8: The structural distribution of the studied inhibitors and their functional groups.

(a) (b) (c)

Figure 9: Captured Images of Hydrates formed in the absence of corrosion inhibitor.

(a) (b) (c)

Figure 10: Captured Images of Hydrates formed by MP

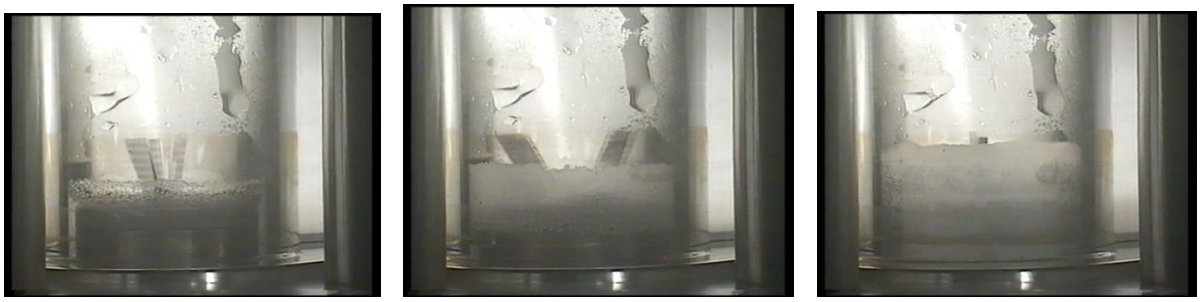

(a) (b) (c)

Figure 11: Captured Images of Hydrates formed by CPC.

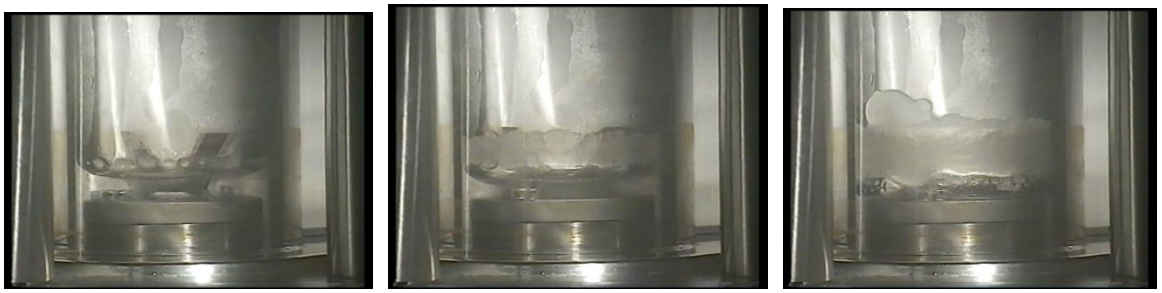

(a) (b) (c)

Figure 12: Captured Images of Hydrates formed by DPC

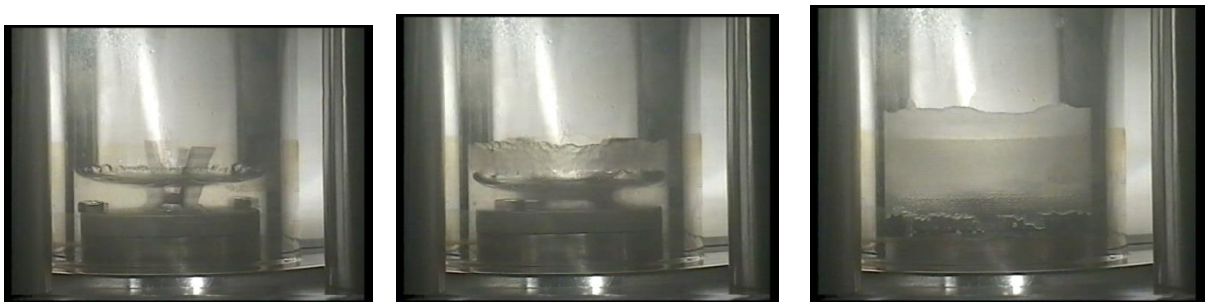

(a) (b) (c)

Figure 13: Captured Images of Hydrates formed by TB

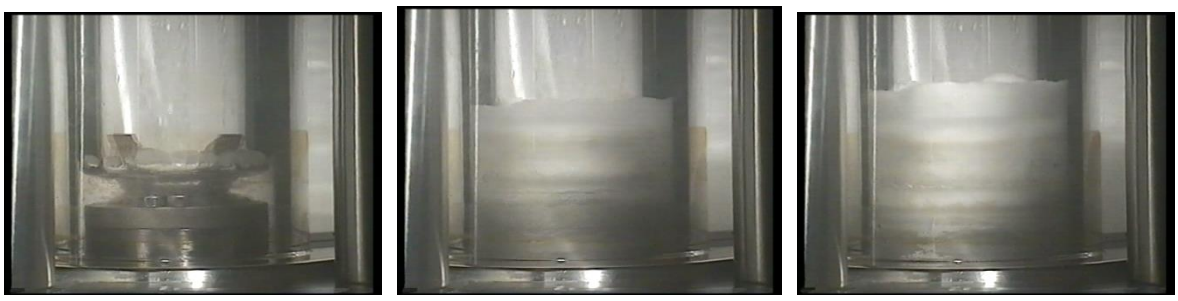

(a) (b) (c)

Figure 14: Captured Images of Hydrates formed by BDHC

Beginning of Experiment Growth begins (T = 0 min) Slow growth (T = 7 mins)

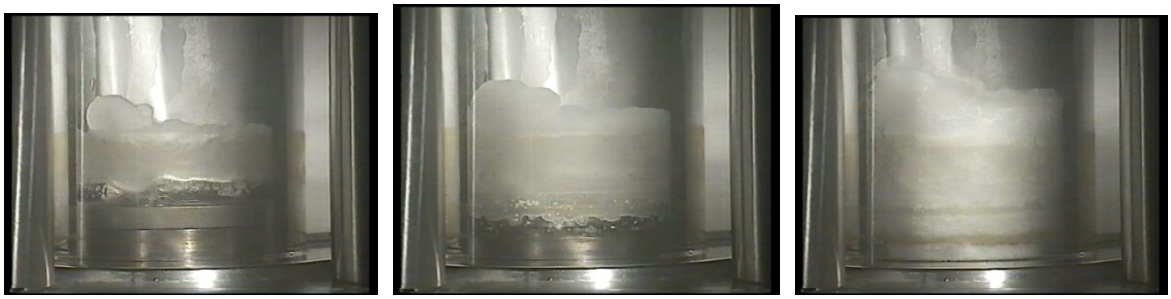

Sudden growth (T = 9 mins) Sharp growth (T = 13 mins) Blockage (T = 14 mins)

Figure 15: Images showing the hydrate growth at 100bar and 500ppm.

1000ppm 2000ppm 3000ppm

5000ppm 10000ppm

Figure 16: Foamy ability at 100bar: It decreases with concentration except at 5000ppm.

Towards blockage At blockage During dissociation

Figure 17: Images showing the foamy growth with time at 3000ppm and 150bar.

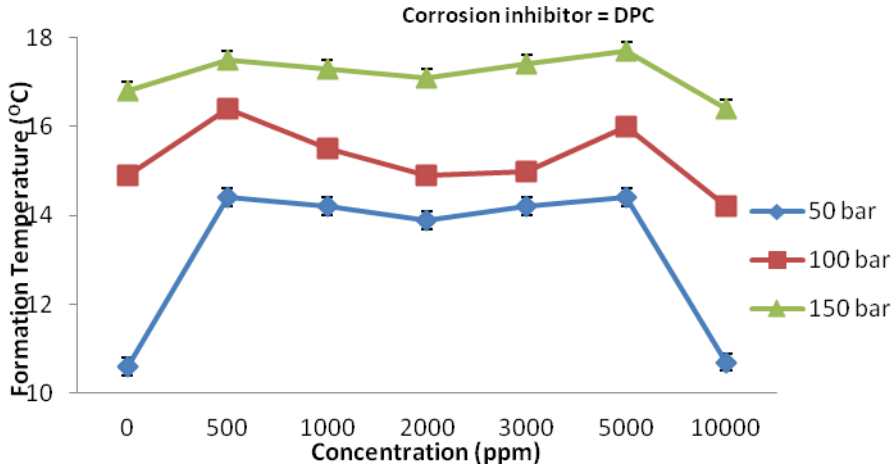

Figure 18: Concentration–pressure matrix showing similar structure at different pressure.

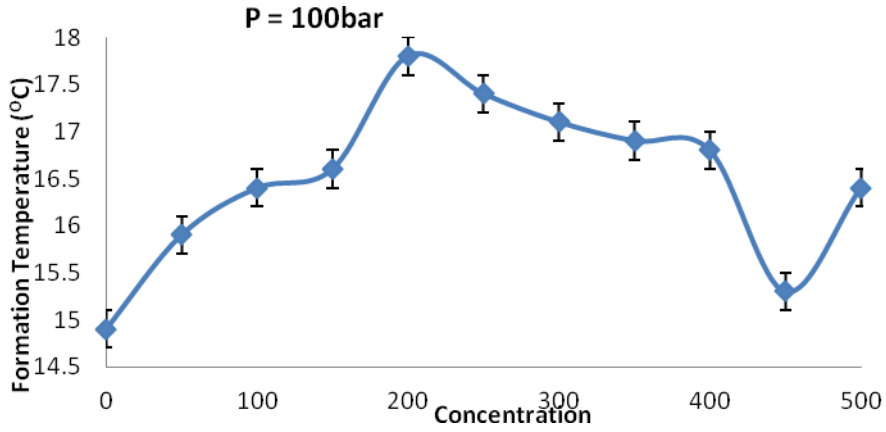

Figure 19: Result establishing the peak concentration for CPC as 200ppm.

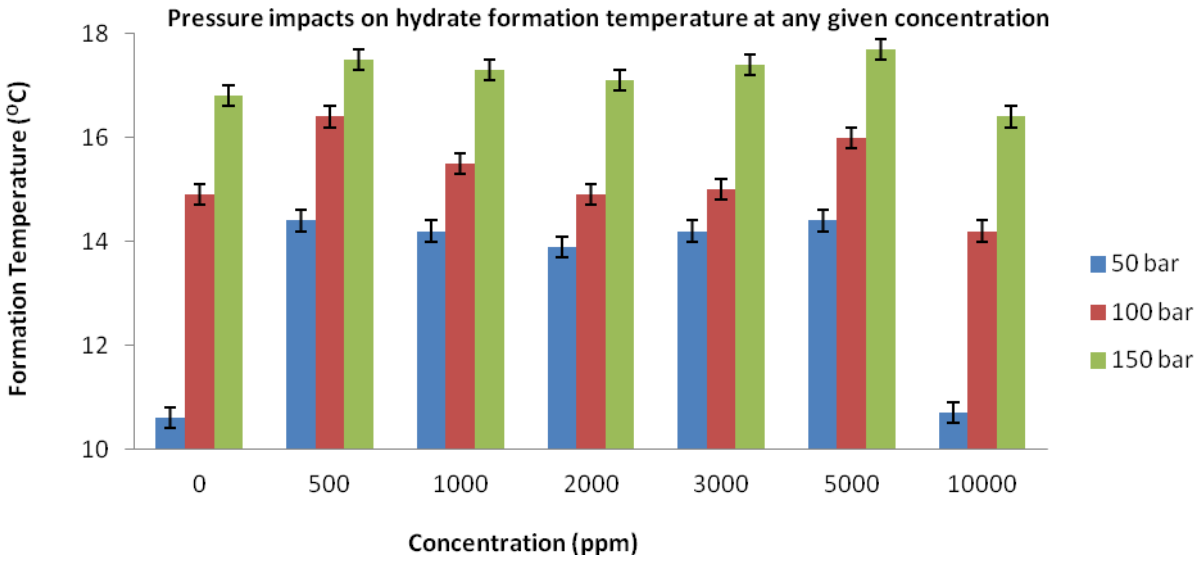

Figure 20: Pressure impacts on hydrate formation temperature at any given concentration.

Figure 21: Hydrate growth trend 1000ppm at 50bar

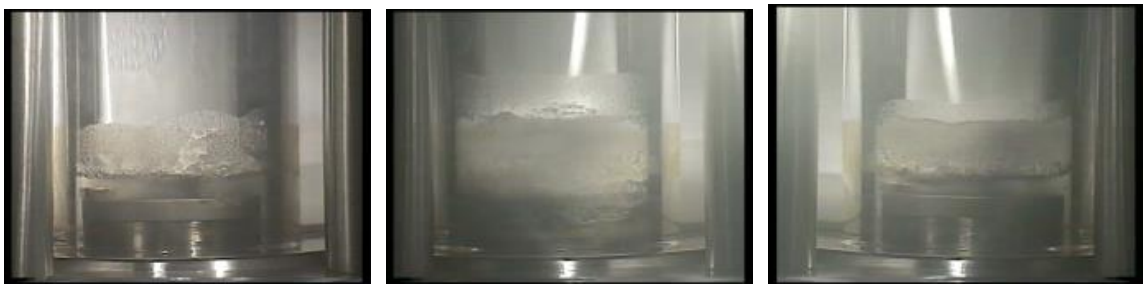

(a) 3000ppm and 100bar (b) 5000ppm and 100 bar (c) 5000ppm and 150 bar

(d) 10000ppm and 100bar (e) 10000ppm and 150bar

Figure 22: Formation of flocs in the liquid phase and hydrate growth in gas phase.

Initial stage Collapsed Rebuilding

Growing Growing Blockage

Figure 23: The collapsing and rebuilding trend at 100bar-10000ppm